JAAS

ROYAL SOCIETY OF CHEMISTRY

PAPER

View Article Online
View Journal | View Issue

Check for updates

Cite this: J. Anal. At. Spectrom., 2023, 38, 950

High-precision measurement of Cd isotopes in ultra-trace Cd samples using double spike-standard addition MC-ICP-MS†

Hui Chang, [a] Jian-Ming Zhu, *[ac] Xiangli Wang [b] and Ting Gao [c]

The double spike-standard addition (DSSA) is a powerful method proposed for isotope measurement of ultra-trace elements in samples. Here, we test the method's practicality and robustness for obtaining high-precision $\delta^{114/110}$Cd data in samples with complex matrices and ultra-trace cadmium (Cd) concentrations as low as 0.004 μg g^{-1}. Through a DS data reduction routine and isotope binary mixing model, the $\delta^{114/110}$Cd values obtained for numeral geological and biological reference materials (GRMs/BRMs) agree well with certified or previous measurements, even for ~2.1 ng Cd of BCR-2. The overall precision of both single- and multi-standard addition depends on the sample fraction (f_{spl}) owing to the error propagation. And 0.041 ± 0.022‰ (2SD, n = 46) of precision for $\delta^{114/110}$Cd can be achieved when the sample fraction (f_{spl}) is ≥20%, comparable to 0.056 ± 0.039‰ (2SD, n = 23) obtained by the traditional DS method. However, it becomes greater than 0.110‰ when f_{spl} is <20%, indicating that 20% (1/5) −50% (1/2) of f_{spl} is the optimal mixing range to obtain high-precision data if the minimal sample sizes are required. These further confirm that accurate and precise Cd isotope ratios can be determined by DSSA. Correspondingly, the purification scheme can be simplified to a single column due to the added standard solution boosting analyte and diluting ratios of matrix/Cd. Animal organs, with 0.004–0.106 μg g^{-1} Cd, yield large variations of $\delta^{114/110}$Cd (−0.054 ± 0.030‰ (2SD, n = 4) and 0.681 ± 0.022‰ (2SD, n = 4) for ovine liver and kidney, respectively), suggesting that Cd isotopes can be fractionated significantly during biological metabolic processes and may be a potential use in medical diagnosis. Robust measurement of Cd isotope composition in ultra-trace Cd samples with complex matrices by DSSA broadens the scope of measurable samples by the traditional DS method, thus potentially opening a range of new opportunities in life, agricultural, environmental, and earth/planetary sciences.

Received 18th February 2023
Accepted 28th February 2023

DOI: 10.1039/d3ja00047h

rsc.li/jaas

1. Introduction

Cadmium (Cd) is a group II-B element located in the fifth period of the periodic table. It usually exists in bivalent Cd(II) in the natural environment and is a toxic metal element with eight stable isotopes (^{106}Cd, ^{108}Cd, ^{110}Cd, ^{111}Cd, ^{112}Cd, ^{113}Cd, ^{114}Cd, and ^{116}Cd). Cadmium is of primary concern in environmental science because of its high mobility from soil to plant and high toxicity to humans.[1,2] However, it also acts as a micronutrient promoting phytoplankton growth by substituting Zn in marine organisms.[3] Cadmium isotopes were first employed in studying planetary evolution as early as the 1970s based on the premise that evaporation and condensation of Cd were the key factors driving Cd isotope fractionation.[4,5] In recent decades, benefiting from technological advancements in multiple-collector inductively couple plasma mass spectrometry (MC-ICP-MS) and multiple-collector thermal ionization mass spectrometers (MC-TIMS), the measurement precision of Cd isotopes ($\delta^{114/110}$Cd) has been improved to 0.030–0.15‰ (2 standard deviation, 2SD).[6–17] Thus, Cd isotopes have been developed as a powerful proxy for constraining oceanic primary productivities,[18–22] reconstructing the biological extinction and anoxic evolution in paleo-environment,[23–26] deciphering the sources and transport pathways of Cd in the surface environment,[27] and understanding the mechanisms of Cd uptake, transport, and accumulation in biological samples.[28–31]

[a]State Key Laboratory of Geological Processes and Mineral Resources, China University of Geosciences (Beijing), Beijing 100083, China. E-mail: jmzhu@cugb.edu.cn; Tel: +86-010-82322832

[b]Key Laboratory of Cenozoic Geology and Environment, Institute of Geology and Geophysics, Chinese Academy of Sciences, Beijing 100029, China

[c]State Key Laboratory of Environmental Geochemistry, Institute of Geochemistry, Chinese Academy of Sciences, Guiyang 550081, China

† Electronic supplementary information (ESI) available: The detailed uncertainty calculation (TEXT S1), instrumental parameters (Table S1), $\delta^{114/110}$Cd values of RMs calculated by DSSA (Table S2), comparison of Cd isotope data calculated by single- and multi-standard methods for GRMs (Fig. S1) and BRMs (Fig. S2), the effects on removing matrix elements by DSSA (Fig. S3) and the calculated $\delta^{114/110}$Cd values of ovine and pig organs (Fig. S4). See DOI: https://doi.org/10.1039/d3ja00047h

However, since Cd content in igneous rocks such as peridotite (0.05 μg g^{-1}), basalts (0.15 μg g^{-1}), and granite (0.10 μg g^{-1}) is commonly lower,[32] its contents of Earth's continental crust and primitive mantle have been estimated to be 0.13 μg g^{-1} and 0.04 μg g^{-1}, respectively.[33–36] Additionally, Cd concentration in animal and human organs is also characterized by trace levels, usually less than 0.07 μg g^{-1},[37–39] except for itai–itai disease patients with ~60 μg g^{-1} Cd in the liver and kidney.[40] Furthermore, even though the amount of Cd required for high-precision Cd isotope measurement has been reduced to ~20 ng,[8,9] large masses of low-Cd samples (*e.g.*, ~5 g rock[32,41] or ~20 L seawater[42]) still need to be processed. Consequently, challenges remain in determining the Cd isotopes of these ultra-trace Cd samples, which impeded the further applications of Cd isotopes in understanding the evolution of Earth's mantle and continental crust, biological metabolic processes, *etc.*

In effort to achieve high-precision measurement of Cd isotopes in those ultra-trace Cd samples, two approaches should be performed as suggested for chromium (Cr) isotopes in Wu *et al.*[43] (1) separate Cd from large mass samples with a more complex purification scheme with sufficiently low blank; (2) improve instrument sensitivity for a smaller sample size. Currently, procedural Cd blank has been decreased to 0.2–30 pg,[8,10,11,13–16] and a Cd mass of 20–100 ng is sufficient to determine Cd isotopes when using an improved sample introduction system (Aridus II desolvator equipped with ice chamber) or higher-impedance Faraday cups (*e.g.*, 10^{13} Ω amplifier).[8,13,14,17] With these setups, the precision has been improved from approximately 0.2‰ to 0.050‰ for $\delta^{114/110}$Cd,[8,9,14,41] even to 0.030‰ when using DS MC-TIMS.[41] Despite all these improvements, the requirement of large amounts of samples for purification still hampers high-sensitivity measurement of Cd isotopes in ultra-trace Cd samples.[8,9,14]

Recently, an innovated technique for analyzing isotopes in ultra-trace element samples, named a double spike-standard addition (DSSA), has been proposed.[44] The key idea of the DSSA technique is the addition of certified standard solution containing DS (*e.g.*, ^{111}Cd–^{113}Cd) with known isotope composition to a sample to boost the amount of analyte. This method only needs ~1/5 of sample mass required for traditional DS while achieving comparable or better precision,[44] which sheds light on measuring Cd isotopes precisely for those naturally ultra-trace Cd samples because the Cd mass of sample for purification can be decreased significantly by adding a DS spiked standard solution. However, although the DSSA's reliability was verified through the pure Cd standard solutions and high-Cd geological reference materials (*e.g.*, NIST 2711a and JSd-2),[44] its application to ultra-trace Cd samples needs to be further tested with more natural samples with various types of matrices to ensure the accuracy and precision is widely applicable.

In order to ground truth of the DSSA and to evaluate its extensive practicality, we subject the DSSA method to tests by a wide variety of samples with ultra-trace Cd concentrations and various matrices. We aim to: (1) confirm the operability of DSSA by showing the detailed procedures, (2) validate Cd isotope accuracy and precision of the essentially ultra-trace Cd samples, and (3) determine Cd isotopes in animal organ samples to test the feasibility of Cd isotopes in medical applications.

2. Experimental methods

2.1. Chemical reagents and materials

All utilized optima-grade nitric acid (HNO_3), hydrochloric acid (HCl) and hydrofluoric acid (HF) (bought from Beijing Institute of Chemical Reagents, China) were distilled once in a sub-boiling distiller (DST-4500, Savillex, USA). Ultrapure water with an 18.2 MΩ cm^{-1} resistivity was obtained through a Milli-Q Element system (Millipore, USA). Thirty-five percent (v/v) H_2O_2 (trace metal grade) was bought from Alfa Aesar. The anion exchange resin AGMP-1M (100–200 mesh) was purchased from Bio-Rad, USA. The Cd standard solution NIST SRM 3108 (lot. 130116) was acquired from the National Institute of Standards and Technology (NIST), USA, and Münster Cd was generously provided by Prof. Rehkämper at Imperial College London (ICL) and Dr Wombacher at University of Cologne. BAM-I012 and SPEX Cd-CUGB were purchased from the Federal Institute for Materials Research and Testing, Germany (BAM) and Merck, China, respectively. The geological and biological reference materials (GRMs/BRMs) were obtained from the United States Geological Survey (USGS) and the Institute of Geophysical and Geochemical Exploration, Chinese Academy of Geological Sciences (CAGS). The GRMs determined in this study include basalt (BHVO-2 and BCR-2), manganese (Mn) nodule (NOD-A-1), river sediment (GSD-12 and GSS-4), marine sediment (MS-E1), and loess (GSS-25). The BRMs included human hair (GSH-1), shrub leaves (GSV-2), wheat flour (GBW08503C) and pig liver (GSB-29). All GRMs and BRMs are listed in Table 1. Actual animal samples, such as liver, kidney, lung of ovine and pig, as well as oysters selected in our experiments, were randomly purchased from supermarkets in Beijing. Rice was collected from the Pb–Zn mining areas in Hezhang County, Guizhou Province, China.

2.2. Preparation of spiked secondary standard solutions

The DSSA includes single- and multi-standard addition approaches. Whether single- or multi-standard addition, it refers to the addition of a pure spiked (containing DS ^{111}Cd–^{113}Cd) Cd standard solution, with known Cd isotope composition, into a sample to boost the amount of analyte. Thus, the spiked secondary standard solutions were made by mixing spiked NIST 3108 with unspiked Münster Cd ($\delta^{114/110}$Cd = 4.461 ± 0.047‰ in our lab[8]) and Spex Cd-CUGB ($\delta^{114/110}$Cd = −2.113 ± 0.041‰[9]). According to the theory of DSSA and an optimal ratio of $^{111}Cd_{spike(spk)}/^{112}Cd_{sample(spl)}$ provided by Tan *et al.*[8] the recommended mixing range of the $^{111}Cd_{spk}/^{112}Cd_{spl}$ was 2–6.[8,44] For Münster-mixed solutions, a $\delta^{114/110}$Cd of 0.489 ± 0.015‰ (2SD) (named $Std1_{Mu}$, $P_{standard(std)}$ = 4.132) was achieved by mixing 10.40% Münster Cd and 89.60% of NIST 3108 ($^{111}Cd_{spk}/^{112}Cd_{spl}$ = 4.621), and a $\delta^{114/110}$Cd value of 0.283 ±

Table 1 The $\delta^{114/110}$Cd values of reference materials determined by DSSA in this study and the literature

Sample name	Sample type	Cd (μg g^{-1})	Used mass (ng, proportion)[a]	Spiked standard solution mass[b]	$\delta^{114/110}$Cd (‰)	σ_{spl} (‰)	$\sigma_{\delta\text{-spl}}$ (‰)	2SD (‰)	N	Sample size (mg)
BCR-2	Basalt	0.18	18.49 (48.03%)	$STD1_{Spex}$ (20 ng)	−0.022	0.018	0.034	0.039	3	102.7
			4.72 (15.88%)	$STD1_{Spex}$ (25 ng)	0.017	0.024	0.120	0.122	3	26.21
			4.99 (16.63%)	$STD1_{Mu}$ (25 ng)	0.010	0.018	0.117	0.119	3	27.71
			2.09 (17.26%)	$STD1_{Mu}$ (10 ng)	−0.015	0.010	0.113	0.113	2	11.59
				Multi-standard (48.03% for $STD1_{Spex}$ and 16.63% for $STD1_{Mu}$)	0.012	0.020	0.110	0.112	9	
				Multi-standard (15.88% for $STD1_{Spex}$ and 16.63% for $STD1_{Mu}$)	0.014	0.012	0.193	0.194	9	
		0.18	30	DS[9]	0.008			0.074[e]	3	166.7
		0.18	25	DS[e] (ref. 8)	−0.030			0.077	4	136.4
		0.22	1000	DS[13]	0.018			0.067	8	4545
		0.21	200–600	DS[32]	0.080			0.040	4	1000–3000
BHVO-2	Basalt	0.086	8.75 (46.67%)	$STD1_{Mu}$ (10 ng)	0.007	0.014	0.029	0.032	4	101.8
			4.48 (14.61%)	$STD1_{Mu}$ (25 ng)	0.035	0.011	0.135	0.137	3	49.75
			9.25 (48.05%)	$STD1_{Spex}$ (10 ng)	0.036	0.013	0.045	0.047	4	107.5
			4.29 (14.64%)	$STD1_{Spex}$ (25 ng)	0.043	0.017	0.131	0.132	3	48.85
				Multi-standard (48.05% for $STD1_{Spex}$ and 46.67% for $STD1_{Mu}$)	0.017	0.014	0.024	0.028	16	
				Multi-standard (14.64% for $STD1_{Spex}$ and 14.61% for $STD1_{Mu}$)	0.024	0.012	0.198	0.199	9	
				Total average[c]	0.018	0.022	0.033	0.046	42	
		0.09	30	DS[9]	0.021			0.074	6	**333.3**
		0.09[d]	30	DS[8]	−0.031			0.077	4	**333.3**
		0.09	100	DS[13]	0.039			0.047	14	1111
		0.152	200	DS[14]	0.040			0.077	2	1316
		0.085	200–600	DS[32]	0.090			0.080	6	800–3000
NOD-A-1	Mn-nodule	6.17	21.22 (51.47%)	$STD1_{Mu}$ (20 ng)	0.133	0.024	0.029	0.038	3	3.44
			24.56 (55.12%)	$STD1_{Spex}$ (20 ng)	0.126	0.014	0.020	0.024	3	3.98
		6.13	30	Multi-standard	0.135	0.015	0.019	0.024	9	
		6.13	30	Total average	0.132	0.017	0.023	0.028	15	
		6.13	1000	DS[9]	0.127			0.035	9	4.89
				DS[8]	0.124			0.067	14	4.89
				DS[13]	0.039			0.047		163.1
MS-E1	Marine sediments	0.064	6.57 (39.65%)	$STD1_{Mu}$ (10 ng)	−0.176	0.008	0.047	0.048	4	102.6
			6.48 (39.32%)	$STD1_{Spex}$ (10 ng)	−0.136	0.021	0.046	0.054	4	101.4
				Multi-standard	−0.162	0.016	0.030	0.035	16	
				Total average[c]	−0.160	0.029	0.041	0.051	24	
		0.064	30	DS[9]	−0.168			0.057	9	**468.8**
GSS-4	Stream sediments	0.34	16.76 (45.60%)	$STD1_{Mu}$ (20 ng)	−0.316	0.021	0.036	0.044	4	51.9
			16.76 (45.60%)	$STD1_{Spex}$ (20 ng)	−0.314	0.014	0.052	0.053	3	51.9
				Multi-standard	−0.314	0.010	0.027	0.029	12	
				Total average[c]	−0.314	0.013	0.038	0.040	19	
		0.32	30	DS[8]	−0.308			0.016	3	93.75
GSD-12	Stream sediments	3.78	19.66 (49.58%)	$STD1_{Mu}$ (20 ng)	−0.122	0.016	0.031	0.036	4	5.2
			18.90(48.57%)	$STD1_{Spex}$ (20 ng)	−0.126	0.022	0.042	0.048	3	5
				Multi-standard	−0.123	0.009	0.027	0.028	12	
				Total average[c]	−0.123	0.012	0.033	0.035	19	
		3.78	30	DS[9]	−0.096			0.035	8	7.94
		3.78	30	DS[8]	−0.071			0.060	8	7.94
		3.78	200	DS[14]	−0.080			0.040	2	52.91

Table 1 (*Contd.*)

Sample name	Sample type	Cd ($\mu g\ g^{-1}$)	Used mass (ng, proportion)[a]	Spiked standard solution mass[b]	$\delta^{114/110}$Cd (‰)	σ_{spl} (‰)	$\sigma_{\delta\text{-spl}}$ (‰)	2SD (‰)	N	Sample size (mg)
GSS-25	Loss	0.15	16.08 (44.57%)	$STD1_{Mu}$ (20 ng)	−0.176	0.027	0.042	0.050	3	107.2
			15.31 (43.39%)	$STD1_{Spex}$ (20 ng)	−0.144	0.014	0.051	0.053	3	108.7
				Multi-standard	−0.155	0.010	0.032	0.034	9	
				Total average[c]	−0.157	0.026	0.042	0.057	15	
		0.14	30	DS[9]	−0.093			0.024	12	214.3
GSH-1	Human hair	0.11	6.00 (37.49%)	$STD1_{Mu}$ (10 ng)	−0.326	0.017	0.041	0.045	4	57.35
			6.00 (37.49%)	$STD1_{Spex}$ (10 ng)	−0.312	0.014	0.057	0.059	4	57.35
				Multi-standard	−0.314	0.010	0.041	0.043	16	
				Total average[c]	−0.316	0.011	0.047	0.049	24	
		0.1	30	DS[8]	−0.377			0.043	2	**300**
GSV-2	Plants	0.51	14.93 (42.75%)	$STD1_{Mu}$ (20 ng)	0.116	0.023	0.027	0.045	4	29.28
			14.93(42.75%)	$STD1_{Spex}$ (20 ng)	0.117	0.005	0.027	0.032	4	29.28
				Multi-standard	0.119	0.011	0.025	0.027	16	
				Total average[c]	0.116	0.013	0.030	0.033	24	
		0.52	30	DS[8]	0.080			0.077	4	57.69
GBW08503C	Wheat flour	0.19	19.21 (49.01%)	$STD1_{Mu}$ (20 ng)	0.103	0.018	0.031	0.035	3	101.1
			19.21(49.01%)	$STD1_{Spex}$ (20 ng)	0.106	0.033	0.043	0.046	3	101.4
				Multi-standard	0.090	0.014	0.026	0.030	9	
				Total average[c]	0.096	0.023	0.033	0.042	15	
		0.18	30	DS[9]	0.107			0.035	9	166.7
GSB-29	Pork liver	0.99	20.77 (50.95%)	$STD1_{Mu}$ (20 ng)	−0.621	0.012	0.025	0.028	3	20.98
			20.77 (50.95%)	$STD1_{Spex}$ (20 ng)	−0.620	0.017	0.038	0.041	3	20.98
			20.77 (50.95%)	$STD2_{Mu}$ (20 ng)	−0.580	0.013	0.037	0.043	3	20.98
			20.77 (50.95%)	$STD2_{Spex}$ (20 ng)	−0.616	0.015	0.051	0.052	3	20.98
				Multi-standard	−0.619	0.053	0.001[f]	0.055	54	
				Total average[c]	−0.618	0.050	0.030	0.059	66	
		0.99	30	DS[9]	−0.611			0.069	9	30.3

[a] The mass (ng) used for purification and its proportion in the mixed solution. [b] The content in the brackets is the amount of standard solution added. [c] Total average is calculated by single- and multi-standard addition, and 2SD is also calculated by the eqn (4), where $\sigma_{\delta\text{-spl}}$ is the average values of error propagation from single-standard and multi-standard methods, excluding the sample data of $f_{spl} \approx 15\%$. [d] This value was an editorial error in Tan *et al.* (2020), which is corrected here. [e] The precision of traditional DS was calculated from the data reported by previous literatures. [f] The error propagation of quadruple-standard addition was calculated by Software MATLAB (2016a).

0.021‰ (named $Std2_{Mu}$, $P_{std} = 2.066$) was obtained by mixing 5.21% Münster Cd and 94.79% NIST 3108 ($^{111}Cd_{spk}/^{112}Cd_{spl} = 2.180$). For Spex-mixed solutions, similar procedures were conducted. A $\delta^{114/110}$Cd of -0.531 ± 0.014‰ (named $Std1_{Spex}$, $P_{std} = 4.111$) and -0.273 ± 0.033‰ (named $Std2_{Spex}$, $P_{std} = 2.051$) were achieved by mixing 25.50% of Spex Cd-CUGB and 74.50% of spiked NIST 3108 ($^{111}Cd_{spk}/^{112}Cd_{spl} = 5.518$), and 13.11% Spex Cd-CUGB and 86.89% of spiked NIST 3108 ($^{111}Cd_{spk}/^{112}Cd_{spl} = 2.360$), respectively.

2.3. Sample digestion and purification

Fresh animal and rice samples were rinsed repeatedly with MQ water to remove adsorbed materials. They were then frozen for 24 hours at −20 °C before being placed in a freeze-dryer to dry to a constant weight. The dried samples were broken into fine particles using ceramic scissors and then stored in sealed bottles to avoid contamination and moisture.

All samples (geological and biological) were decomposed following the procedures described in Zhu *et al.*[45] Briefly, approximately 50 mg of basalt samples was placed in a 15 mL PFA beaker with 2 mL of HF and 1 mL of HNO_3, sealed, heated at 150 °C on a hot plate for 8–10 h, and then evaporated. Aqua regia (4 mL; HCl : HNO_3 = 3 : 1) was then added and heated for 8–10 h until the samples were completely dissolved. For soil and sediment samples, approximately 100 mg of powder sample was weighed into 30 mL Teflon (PTFE) liner vials. Then, 0.6 mL HF and 2.6 mL HNO_3 were added. After heating at 180 °C for 36–48 h in a pre-heated oven, the samples were evaporated to incipient dryness and the above procedures were repeated. For plant and animal samples, 100–200 mg was weighed into 30 mL PTFE. Then, 3 mL HNO_3 was added for degassing 2 h and then heated at 180 °C for 16 h before being evaporated to dryness. Finally, all samples were dissolved in 10% HNO_3 (v/v) as stock solutions. Due to high organic contents, animal samples (*e.g.*, oyster shell) were digested in several parallel aliquots and recombined after each complete digestion.

Before purification, samples containing approximately 2.09–30 ng Cd were mixed with an appropriate amount (proportion 20–80%, w/w) of the spiked secondary standard solutions in 15 mL of PFA, sealed, and heated on a hotplate overnight at 100 °C to ensure that the mixed solutions were homogeneous. Samples were dissolved by adding 2 mL of 2 M HCl after evaporation and loaded onto a clean column containing 3 mL of AGMP-1M resin which

were conditioned with 2 M HCl, followed by 2 M, 1 M, 0.3 M and 0.06 M HCl.[8] Finally, Cd was eluted and collected with 0.0012 M HCl. The above steps were repeated twice for DS and once for DSSA to obtain high-purity Cd for isotope measurement.

2.4. Cd content and isotope measurement

The initial Cd contents of biological samples were determined by high-resolution (HR)-ICP-MS (Element-XR, ThermoFisher, U.S.A.) at the Isotope Geochemistry Laboratory (IGL-CUGB), China University of Geosciences (Beijing), and the actual Cd contents was corrected by the double spike method.[9] The Cd isotopes were determined on a MC-ICP-MS (Neptune Plus, ThermoFisher, U.S.A.) at IGL-CUGB and the instrumental parameters were similar to those reported in Tan *et al.*[8] (Table S1†) to ensure that the ^{112}Cd signal was maximized. The purified solution was diluted to 5–10 ng mL^{-1} using 2% HNO_3 + 0.1% HF and introduced into the plasma *via* an improved Aridus II desolvator with an ice chamber.[43] NIST SRM 3108 was analyzed every 4–5 samples before and after to monitor instrument shift or stability, and then they were used to normalize the sample data. Each sample was repeatedly measured 3–4 times in the different analytical sessions to achieve the actual 2SD (external reproducibility: $\sigma_{external}$) used in calculating the data precision of the samples. The $\delta^{114/110}$Cd was expressed relative to NIST 3108 as eqn (1).

$$\delta^{114/110}\mathrm{Cd} = \left(\left(^{114}\mathrm{Cd}/^{110}\mathrm{Cd}\right)_{sample}/\left(^{114}\mathrm{Cd}/^{110}\mathrm{Cd}\right)_{NIST3108} - 1\right) \times 1000 \quad (1)$$

2.5. Data reduction

DSSA can be done with a single standard or can be repeated with multiple standards (with different known Cd isotope compositions) to cross-validate results. The $\delta^{114/110}Cd_{std}$ represents the Cd isotope compositions of the spiked secondary standard solution, which was certified by long-term measurement. The $\delta^{114/110}Cd_{spl}$, $\delta^{114/110}Cd_{mix}$ (mixed solution: std + spl), $P_{std}(^{111}Cd_{spk}/^{112}Cd_{std})$, and $P_{mix}(^{111}Cd_{spk}/^{112}Cd_{mix})$ can be precisely achieved by DS data reduction Worksheet. For a single-standard, the $\delta^{114/110}$Cd value of an unknown sample can be solved by eqn (2):[44]

$$\delta^{114/110}Cd_{spl} = (P_{std} \times \delta^{114/110}Cd_{mix} - P_{mix} \times \delta^{114/110}Cd_{std})/(P_{std} - P_{mix}) \quad (2)$$

The uncertainty of calculated δ_{spl} comes from the errors associated with the P and δ values of the standard and mixed solutions. Error propagation can be calculated by eqn (3).[44]

$$\sigma_{\delta\text{-spl}} = \frac{\sqrt{P_{mix}{}^2\sigma_{\delta\text{-std}}{}^2 + P_{std}{}^2\sigma_{\delta\text{-mix}}{}^2}}{P_{std} - P_{mix}} \quad (3)$$

where $\sigma_{\delta\text{-std}}$ and $\sigma_{\delta\text{-mix}}$ are the 2SDs of the measured standard and mixed solutions, respectively. Here, the uncertainty of all data is expressed as 2SD, and the overall precision was calculated by the average error propagation of multiple measurements of the single mixed sample solution and its external reproducibility, as provided by Schoenberg *et al.*[46]

$$2\mathrm{SD} = \sqrt{(\sigma_{external})^2 + (\sigma_{\delta\text{-spl}})^2} \quad (4)$$

where $\sigma_{external}$ represents the external reproducibility of each sample, obtained by ≥3 times analytical results.

For multi-standard approach, sample solutions are mixed with two or more spiked secondary standard solutions with different known Cd isotope compositions. These mixed solutions generate a series of two-end member mixing lines. These lines ideally should intersect at one point for a sample, which defines the true Cd isotope composition of the unknown sample. However, due to analytical uncertainties or the weak drift during analytical sessions, these (or regression) line themselves may generate multiple intersections.

The number of intersections can be calculated as $n_1 \times n_2 + n_3 \times (n_1 + n_2) + n_4 \times (n_1 + n_2 + n_3)\ldots$ (where n_1, n_2, n_3, and $n_4\ldots$ were the analysis times of the corresponding single-standard). For instance, four measurements produce four mixed lines using $Std1_{Spex}$, and so do $Std1_{Mu}$ (*e.g.*, Fig. S1b†). The total intersections should be $4(n_1) \times 4(n_2) = 16$. When the third ($Std2_{Mu}$) or fourth ($Std2_{Spex}$) spiked standard solution was employed and each was measured 3 times (*e.g.*, Fig. S2a†). The total intersections should be $3(n_1) \times 3(n_2) = 9$ for double ($Std1_{Mu}$ and $Std1_{Spex}$), $3(n_1) \times 3(n_2) + 3(n_3) \times (3 + 3) = 27$ for ternary and $3(n_1) \times 3(n_2) + 3(n_3) \times (3 + 3) + 3(n_4) \times (3 + 3 + 3) = 54$ for quadruple-standard addition. Then, the $\delta^{114/110}$Cd value and uncertainty of an unknown sample can be acquired by solving intersections of regression lines using eqn (5) and (6) for double-standard addition.

$$\delta^{114/110}Cd_{spl\text{-}multi} = \frac{P_{std1} \times \left(\delta^{114/110}Cd_{std1} - \delta^{114/110}Cd_{mix1}\right) \times \left(\delta^{114/110}Cd_{std2} - \delta^{114/110}Cd_{std1}\right)}{(P_{std2} - P_{mix2}) \times P_{std1} \times \left(\delta^{114/110}Cd_{std1} - \delta^{114/110}Cd_{mix1}\right) - (P_{std1} - P_{mix1}) \times P_{std2} \times \left(\delta^{114/110}Cd_{std2} - \delta^{114/110}Cd_{mix2}\right)} + \delta^{114/110}Cd_{std1} \quad (5)$$

where $\delta^{114/110}Cd_{spl\text{-}multi}$ is the calculated values from multi-standard method, $\delta^{114/110}Cd_{std1}$, $\delta^{114/110}Cd_{std2}$ are the Cd isotope composition of the different spiked secondary standard solutions such as $Std1_{Mu}$ and $Std1_{Spex}$. $\delta^{114/110}Cd_{mix1}$ and $\delta^{114/110}Cd_{mix2}$ are the Cd isotope composition of the sample mixed with Std1 and Std2, respectively. P_{std1}, P_{std2}, P_{mix1}, and P_{mix2} denotes $^{111}Cd_{spk}/^{112}Cd_{std/mix}$ of Std1, Std2, mix1, and mix2, respectively.

The error propagation can be estimated by the following equation:

$$\sigma_{\delta spl\text{-}multi} = \sqrt{\begin{aligned}&\left(\frac{\partial_{\delta spl\text{-}multi}}{\partial_{\delta std1}}\right)^2 \times {\sigma_{\delta std1}}^2 + \left(\frac{\partial_{\delta spl\text{-}multi}}{\partial_{\delta std2}}\right)^2 \times {\sigma_{\delta std2}}^2 + \left(\frac{\partial_{spl\text{-}multi}}{\partial_{\delta mix1}}\right)^2 \times {\sigma_{\delta mix1}}^2 + \\ &\left(\frac{\partial_{\delta spl\text{-}multi}}{\partial_{\delta mix2}}\right)^2 \times {\sigma_{\delta mix2}}^2 + \left(\frac{\partial_{\delta spl\text{-}multi}}{\partial_{Pstd1}}\right)^2 \times {\sigma_{Pstd1}}^2 + \left(\frac{\partial_{\delta spl\text{-}multi}}{\partial_{Pstd2}}\right)^2 \times {\sigma_{Pstd2}}^2 + \\ &\left(\frac{\partial_{\delta spl\text{-}multi}}{\partial_{Pmix1}}\right)^2 \times {\sigma_{Pmix1}}^2 + \left(\frac{\partial_{\delta spl\text{-}multi}}{\partial_{Pmix2}}\right)^2 \times {\sigma_{Pmix2}}^2\end{aligned}} \quad (6)$$

where $\sigma_{\delta std1}$, $\sigma_{\delta std2}$, $\sigma_{\delta mix1}$ and $\sigma_{\delta mix2}$ represent the two standard deviations (2SD) of δ values of std1, std2, mix1 and mix2, respectively, and $\sigma_{Pstd1}/\sigma_{Pstd2}$ and $\sigma_{Pmix1}/\sigma_{Pmix2}$ denotes the 2SD of P values of standard and mixed solutions, respectively. Each error term derivation is provided in the TEXT S1.†

3. Results and discussion

3.1. Blank contribution

The total procedural blank of Cd from digestion to the end of purification in our experiments is ~23 pg, less than 0.08% of samples containing 30 ng Cd. The blanks from digestion and column procedures are individually 8 ± 6 pg (2SD, $n = 5$) and 7 ± 5 pg (2SD, $n = 5$). For DSSA, the minimum Cd amount in the unknown samples is 1.53 ng. Thus, the digestion, column, and total procedural blank accounts for 0.52%, 0.98% and 1.50% of this sample, respectively. These blanks should be a negligible effect on the $\delta^{114/110}$Cd values.[8] However, to evaluate the blank effect further on the $\delta^{114/110}$Cd in ultra-trace Cd samples, the blank solution from digestion step was mixed with the unprocessed $Std1_{Spex}$ containing 5 ng Cd, which is no effect on the $\delta^{114/110}$Cd (−0.533 ± 0.010‰, 2SD, $n = 3$) of $Std1_{Spex}$. Simultaneously, the $Std1_{Spex}$ containing 5 and 20 ng Cd was purified and measured, yielding $\delta^{114/110}$Cd values of −0.530 ± 0.035‰ (2SD, $n = 3$, determined at 5 ppb injection concentration) and −0.531 ± 0.017‰ (2SD, $n = 5$), respectively, identical within uncertainty to the unprocessed standard ($\delta^{114/110}Cd = -0.531 \pm 0.014$‰; 2SD, $n = 13$). Besides, an aliquot of BCR-2, containing 2.09 ng Cd, was also processed, and its $\delta^{114/110}$Cd is consistent with reported values within the uncertainty.[8,9,13,14,32] Therefore, the blank does not influence the accuracy in the calculated $\delta^{114/110}$Cd values of unknown samples.

3.2. Evaluation of the accuracy and precision

Accuracy and precision are critical indicators of judging data quality. Standard solutions and RMs are typically used to evaluate the precision and accuracy of natural samples. In this study, accuracy was evaluated by comparison with published or certified $\delta^{114/110}$Cd values of RMs. Long-term measurements of NIST SRM 3108, BAM-I012, and Spex Cd-CUGB yielded average $\delta^{114/110}$Cd values of −0.002 ± 0.013‰ ($n = 117$), −1.320 ± 0.032‰ (2SD, $n = 10$), and −2.104 ± 0.017‰ (2SD, $n = 10$), respectively. These data agree well with previously reported values.[7,8,13,18,42,47] For the spiked secondary standard solutions, the measured $\delta^{114/110}$Cd values of $Std1_{Mu}$ and $Std1_{Spex}$ were 0.489 ± 0.015‰ (2SD, $n = 13$) and −0.531 ± 0.014‰ (2SD, $n = 13$), respectively, in agreement with the theoretically calculated values (0.484 ± 0.030‰ and −0.531 ± 0.023‰) using the isotope binary mixing model. These measured values will be used in single- or multi-standard addition approaches of DSSA as an initial endmember in eqn (2).

For the single-standard addition, $\delta^{114/110}$Cd values and their precision of RMs were obtained by eqn (2) and (4). All RMs' $\delta^{114/110}$Cd values are analytically indistinguishable from the reported data (Fig. 1).[8,9,13,14,32] However, it is worth noting that the precision depends strictly on the proportion of sample mass in the mixture owing to the error propagation. As shown in Fig. 2a, when sample fraction (f_{spl}) is close to 15–10% (w/w), our

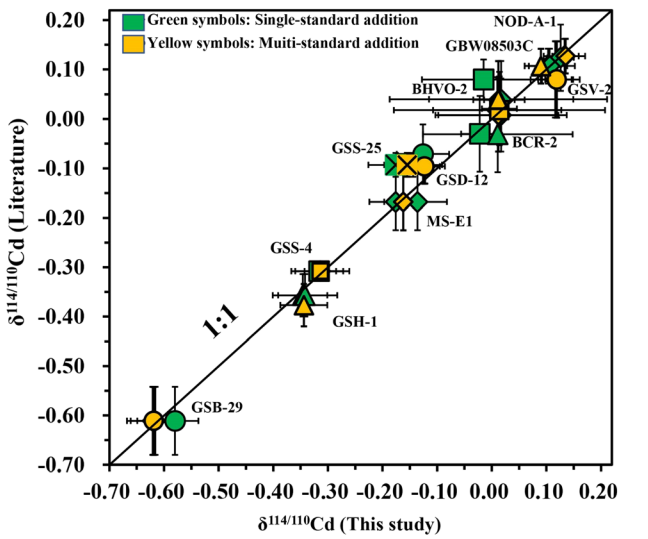

Fig. 1 Comparison of Cd isotope data between this study and traditional DS reported in previuos studies.[8,9,13,14,32] The green and yellow symbols represent $\delta^{114/110}$Cd for single- and multi-standard, respectively.

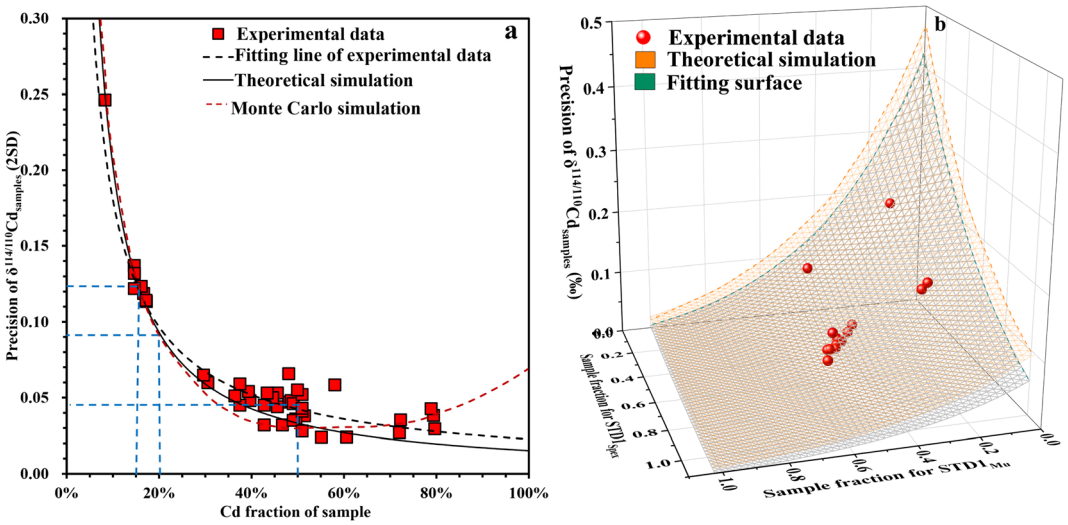

Fig. 2 The relationship between overall precision and sample fraction (f_{spl}) of single-standard (a) and multi-standard (b). The y value of the horizontal blue dashed line is the overall precision, and the x value of the vertical blue dashed line is f_{spl}.

samples' precision becomes relatively large with up to 0.137‰ (BHVO-2: $\delta^{114/110}$Cd = 0.035 ± 0.137‰, Table 1), even up to 0.246‰ when f_{spl} is 8.29% although its accuracy is acceptable (Ovine liver: $\delta^{114/110}$Cd = −0.048 ± 0.246‰, Table 2). This observation is similar to the trend line presented in Lu *et al.*[44] Still, if the f_{spl} is ≥20% as listed in Table 1, the precision can be significantly improved. For example, 2.09 ng of Cd from BCR-2 digest solution was mixed with 10 ng of $Std1_{Mu}$, its proportion (f_{spl}) is 17.26% and the $\delta^{114/110}$Cd is −0.015 ± 0.113‰ (2SD, n = 3). This value is still identical to the published data, but the precision is approximately two times what was previously reported.[8,9,13,32]. The basalt reference material BCR-2 (18.49 ng Cd, f_{spl} = 48.03%) was dopped with $Std1_{Spex}$ (20 ng Cd), yielding a calculated $\delta^{114/110}$Cd value of −0.022 ± 0.039‰ (2SD, n = 3)

Table 2 The $\delta^{114/110}$Cd values of biological materials

Sample type	Cd[a] (μg g^{-1})	Used mass[b] (ng, proportion)	Spiked solution (added ng)	$\delta^{114/110}$Cd (‰)	σ_{spl} (‰)	$\sigma_{\delta\text{-}spl}$ (‰)	2SD	N	Sample size (mg)
Ovine kidney	0.076	30.85 (72.00%)	$STD1_{Mu}$ (12)[c]	0.681	0.016	0.022	0.027	4	408.1
		4.81 (16.13%)	$STD1_{Mu}$ (25)	0.648	0.022	0.121	0.123	3	63.26
		36.25	DS[e]	0.565			0.037	3	477.1
Ovine liver	0.077	39.16 (79.67%)	$STD1_{Mu}$ (10)	−0.054	0.018	0.014	0.030	4	506.0
		2.26 (8.28%)	$STD1_{Mu}$ (25)	−0.048	0.014	0.246	0.246	3	29.34
		30	DS[e]	−0.081					389.6
Ovine lung	0.009	8.58 (36.39%)	$STD1_{Mu}$ (15)	0.101	0.023	0.045	0.051	3	957.2 (3333)[f]
Pig kidney	0.106	38.55 (79.40%)	$STD1_{Mu}$ (10)	0.383	0.027	0.027	0.038	4	365.1 (284.1)
		5.18 (17.16%)	$STD1_{Mu}$ (25)	0.344	0.012	0.114	0.114	3	48.86
		38.31 (78.86%)	$STD1_{Spex}$ (10)	0.370	0.03	0.031	0.043	3	365.3
			Muti-standard	0.381	0.022	0.042	0.048	12	
			Total average[d]	0.370	0.024	0.032	0.040	22	
Pig liver	0.020	13.82 (58.02%)	$STD1_{Mu}$ (10)	0.037	0.038	0.036	0.058	3	694.1
		9.98 (49.95%)	$STD1_{Spex}$ (10)	0.060	0.033	0.044	0.055	3	692.0
			Muti-standard	0.042	0.021	0.042	0.049	9	
			Total average[d]	0.044	0.031	0.031	0.044	15	
		30	DS[e]	0.083			0.010	3	1500
Pig lung	0.011	8.98 (30.57%)	$STD1_{Mu}$ (15)	−0.009	0.018	0.057	0.060	4	816.1 (2724)
Oyster shell	0.004	1.58 (24.01%)	$STD1_{Mu}$ (5.0)	−0.591	0.013	0.020	0.024	4	395.2 (7515)
		10.51 (29.61%)	$STD1_{Mu}$ (25)	−0.608	0.019	0.062	0.065	3	2629
Rice	1.00	32.53 (72.26%)	$STD1_{Mu}$ (15)	0.175	0.022	0.028	0.035	4	32.53
		4.10 (14.64%)	$STD1_{Mu}$ (25)	0.158	0.021	0.120	0.122	3	4.14
			DS[e]	0.159			0.060	3	103.4

[a] Cd content was obtained by DS. [b] The mass (ng) used for purification and its proportion in the mixed solution. [c] The mass in brackets is the amount of standard solution added. [d] Total average is calculated by single- and multi-standard addition. [e] DS is the traditional double-spike method. [f] The sample sizes in brackets are calculated by traditional DS according to the minimum Cd mass of 30 ng used in our laboratory.

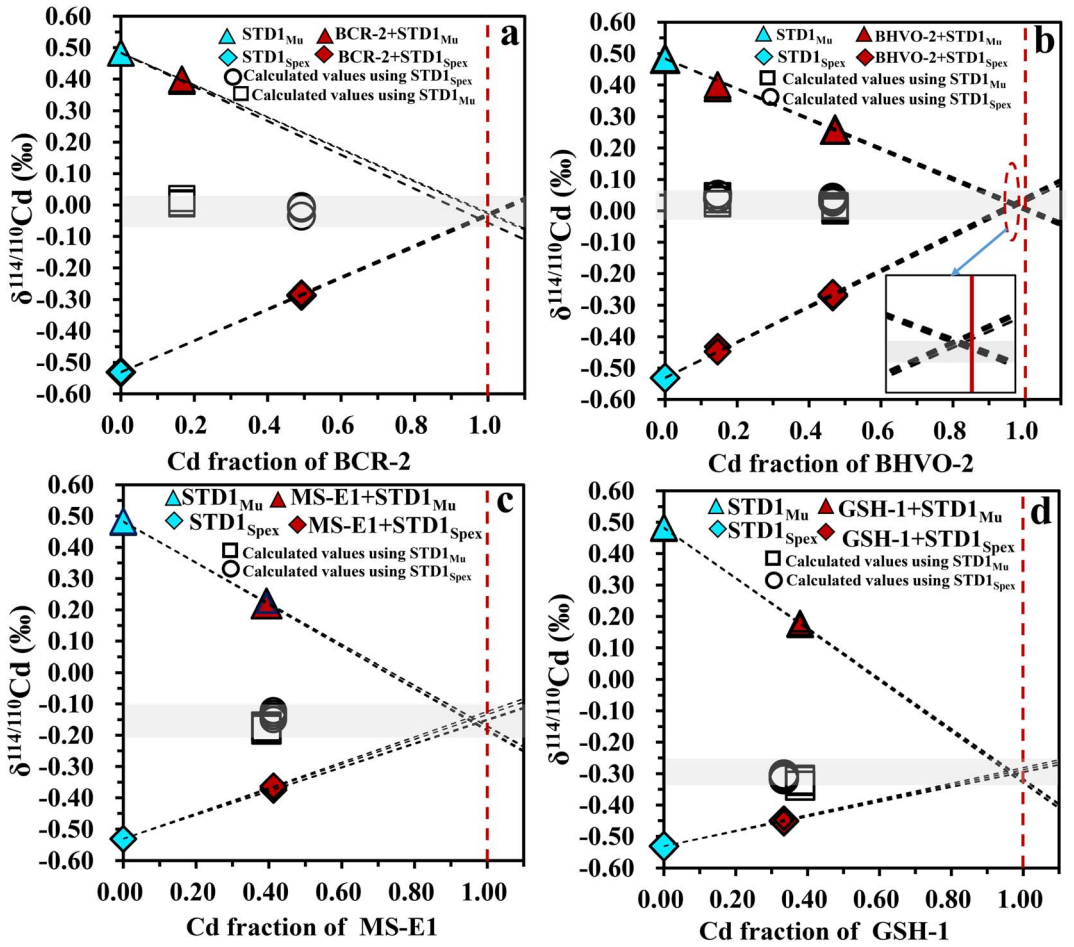

Fig. 3 The $\delta^{114/110}$Cd values of several RMs ((a) BCR-2; (b) BHVO-2; (c) MS-E1; (d) GSH-1) obtained by DSSA. The blue and red triangles are the $\delta^{114/110}$Cd values of $STD1_{Mu}$ and samples mixed with $STD1_{Mu}$, respectively. The blue and red diamonds are the $\delta^{114/110}$Cd values of $STD1_{Spex}$ and samples mixed with $STD1_{Spex}$, respectively. The open circles and squares represent the actual $\delta^{114/110}$Cd values calculated for unknown samples. The black dashed lines are linear fitting lines. The intersection of the fitting lines with the $f_{spl} = 1$ (vertical red dash line) defines the "true" $\delta^{114/110}$Cd value of the sample. The calculated values (open circles and squares) should fall on the horizontal line passing through the "true" value. The gray bar denotes the values (±2SD) measured in Tan *et al.* (2020)[8] and Lu *et al.* (2021).[9]

(Fig. 3a, Tables 1 and S2†). Measurement of BHVO-2 (8.75 ng and 9.25 ng Cd, $f_{spl} = 46.67\%$ and 48.05%) with single-standard addition yielded a $\delta^{114/110}$Cd value of 0.007 ± 0.032‰ (2SD, $n = 4$) using $Std1_{Mu}$ (10 ng Cd) and 0.036 ± 0.047‰ (2SD, $n = 4$) using $Std1_{Spex}$ (10 ng Cd) (Fig. 3b, Tables 1 and S2†), which are consistent with the published values and their corresponding precision.[8,9,13] Similarly, the $\delta^{114/110}$Cd values of NOD-A-1 were 0.133 ± 0.038‰ (2SD, $n = 3$) using $Std1_{Mu}$ and 0.126 ± 0.024‰ (2SD, $n = 3$) using $Std1_{Spex}$ (Tables 1, S2 and Fig. S1a†). For river sediment RMs, the $\delta^{114/110}$Cd of GSS-4 was −0.316 ± 0.044‰ (2SD, $n = 4$) using $Std1_{Mu}$ and −0.314 ± 0.053‰ (2SD, $n = 4$) using $Std1_{Spex}$ (Tables 1, S2 and Fig. S1b†). The results of GSD-12, MS-E1, and GSS-25 using $Std1_{Mu}$ and $Std1_{Spex}$ were almost identical and consistent with reported values and uncertainty (Fig. 3c, S1† and Tables 1, S2†).[8,9] Thus, 20–50% of f_{spl} is the optimal mixing range for Cd isotopes if we want to obtain high-precision data using as small a sample mass as possible.

For the multi-standard addition, similar observation for precision still existed (Fig. 2b). When the f_{spl} is less than 15%, the uncertainty for multi-standard is larger than 0.190‰ (BCR-2: $\delta^{114/110}Cd = 0.014 \pm 0.194$‰, Table 1), while the f_{spl} is close to 50%, the precision for RMs can reach to 0.033 ± 0.017‰ (2SD, $n = 10$, Table 1). For example, the precision of BHVO-2 is 0.199‰ at 14.64% of f_{spl} for $Std1_{Spex}$ and 14.61% of f_{spl} for $Std1_{Mu}$, whereas it can be decreased to 0.028‰ when f_{spl} is 48.05% for $Std1_{Spex}$ and 46.67% for $Std1_{Mu}$ (Table 1). Thus, the optimal mixing range of 20–50% is still applicable to the multi-standard approach. As shown in Table 1 and Fig. 3b, the average $\delta^{114/110}$Cd values obtained from double-standard intersections (each measured four times) were 0.017 ± 0.028‰ (2SD, $n = 4 \times 4 = 16$; Fig. 3b) for BHVO-2 ($f_{spl} \geq 46.67\%$) and −0.314 ± 0.043‰ (2SD, $n = 4 \times 4 = 16$; Fig. 3d) for GSH-1 ($f_{spl} = 37.49\%$), which are identical to published data.[9] The $\delta^{114/110}$Cd values of other GRMs and BRMs obtained from double-standard addition are also consistent with those achieved from single-standard addition as well as with those measured in previous studies (Table 1).[8,9,14] Beside $Std1_{Mu}$ and $Std1_{Spex}$, $Std2_{Mu}$ and $Std2_{Spex}$ were also individually mixed with GSB-29 ($f_{spl} = 50.95\%$). The

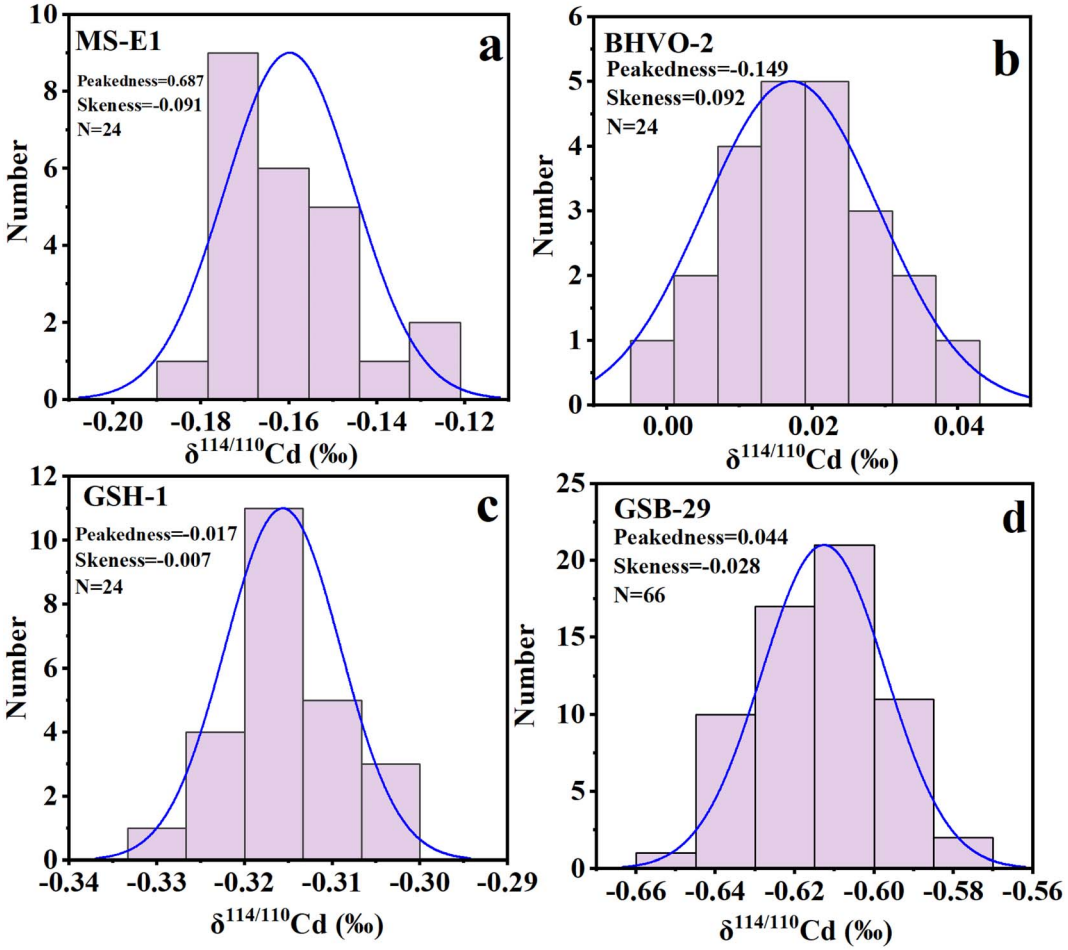

Fig. 4 Normal distribution test for RMs' data ((a) MS-E1; (b) BHVO-2; (c) GSH-1; (d) GSB-29).

$\delta^{114/110}$Cd of -0.619 ± 0.055‰ (2SD, $n = 54$) calculated by quadruple-standard addition is consistent with single-standard addition result (-0.620 ± 0.041‰, $n = 12$). Above comparison with published values shows that both single and multiple standard addition can produce accurate isotope ratio data (Fig. 1).

However, it is necessary to note that, if no systematic errors occur during single- and multi-standard calculation, obtained $\delta^{114/110}$Cd values should conform to normal distribution. For example, the number of intersections was 24 for MS-E1 (Fig. 4a and Table 1), including 16 intersection values by double-standard mixing lines ($n = 16$) and single-standard addition ($n = 8$). Normal distribution tests were performed using Kurtosis/skewness coefficient, P–P plot, and Shapiro–Wilk approaches. Assuming that the data follows normal distribution at the confidence level of 0.05, the hypothesis will be rejected when the Kurtosis and skewness coefficient is >1.96 and the data is not subject to normal distribution. Otherwise, the assumption is valid. All Kurtosis and skewness coefficients are <1.96 for $\delta^{114/110}$Cd values. And P–P plot displays that all data of each sample fall on line with the slope of 1. The Shapiro–Wilk test also gives the same results at the confidence level of 0.05. These observations show that the distribution of all values accords with normal distribution, and so do the others (Fig. 4a–d). Thus, the short-term external reproducibility can be represented by arithmetic mean and standard deviation. The average external precision for single standard addition is 0.019 ± 0.014‰ (2SD, $n = 43$) with range of 0.005 to 0.038‰. And the overall reproducibility of multi-standard is 0.017 ± 0.022‰ (2SD, $n = 15$). Revisiting the uncertainty of all data with considering error propagation, we know the precision ranges from 0.024 to 0.137‰ with an average of 0.059 ± 0.066‰ (2SD, $n = 43$) for single standard addition, whereas it falls within the range of 0.024 to 0.199‰ with an average of 0.062 ± 0.117‰ (2SD, $n = 15$) for multiple standard addition (including double- and quadruple-standard). Obviously, the relatively large precision variation is dominantly coming from the error propagation contribution of f_{spl} (sample fraction) ≈ 15%. Two independent-sample t-tests ($P < 0.05$) show there are no significant difference between them. Thus, excluding the sample data of $f_{spl} \approx 15\%$, the overall precision of DSSA in our work is 0.041 ± 0.022‰ (2SD, $n = 46$), which is comparable with the statistical average value (0.056 ± 0.039‰, 2SD, $n = 23$, Table 1) obtained by the traditional DS method in previous works,[8,9,13,14,32] indicating that the $\delta^{114/110}$Cd values from single- and multi-standard approaches are both robust, and the results in our study are

good in the repeatability and consistency. The $\delta^{114/110}$Cd values of the selected GRMs and BRMs are excellently in line with published data (Table 1).[8,9,13,14,32]

Additionally, since multiple standard addition needs ≥2 spiked standard solution, and its operation is relatively tedious, our results confirm that single-standard addition is sufficient to obtain the reliable data and easier to operate when using DSSA. It should be noted that some intersections of mixing lines do not exactly coincide with the "true value" of the sample (Fig. 3c and d), which is likely due to instrument drift or analytical errors from measurements. However, the intersection values obtained from mixing lines (intersections demarcated in ovals in Fig. 3b) are within analytical uncertainty identical with the calculated values from the single-standard addition (open markers in Fig. 3). The worst precision (0.057‰; $f_{spl} \geq 20\%$) obtained by multiple-standard addition is still comparable with the 0.056 ± 0.039‰ (2SD, $n = 23$, Table 1) of traditional DS.[8,9,13,14,32]

3.3. Feasibility of DSSA for ultra-trace Cd samples

Generally, the loading amount of Cd for chemical purification ranged from 30 to 1000 ng.[8–17,44,45] For ultra-trace Cd GRMs (*e.g.*, BHVO-2 and MS-E1) and natural samples (*e.g.*, peridotites, Cd = 11.5 ng g^{-1}), the minimum sample mass containing 30 ng Cd are approximately 340 mg of BHVO-2 (ref. 8) and 3000 mg of rock powder[32] according to the traditional DS. Whereas for DSSA, according to the recommended optimal range of 20–50% for f_{spl}, precision requirement and blank effect, approximately 60 mg or 600 mg of sample mass is sufficient to extract Cd for isotope measurement because the amount of Cd can be reduced to 6 ng (30 ng × 20%) or lower through optimizing f_{spl}. In our work, the sample mass of BCR-2 and BHVO-2 was used commonly 100 mg while at least 300 or 800 mg is needed in the study of Tan *et al.*[8] and Pickard *et al.*[32] What's more, we still obtained good data using sample mass of ∼12 mg BCR-2 and ∼50 mg BHVO-2 (Table 1). Similarly, for BRMs with ultra-trace Cd (*e.g.*, GSH-1 and GBW080503C), the sample mass can also be reduced to 30–50 mg, a 6-fold reduction compared to those (300 mg) used in Tan *et al.*[8]

With decreased sample consumption and added pure standard solution to boost analyte, the ratios of matrix/Cd, especially Sn/Cd, can be correspondingly decreased by 80–50% of the actual samples. The observation of Sn tailing into Cd cut has been reported in literature,[8] and the positive drift of $\delta^{114/110}$Cd value could occur when Sn/Cd in purified solution is >0.02, which leads to the double separation for traditional DS.[8] In our test experiments, the comparison between DS and DSSA using single column showed that Sn/Cd of GSB-29, GBW08503C and GSV-2 were sometimes higher than 0.02 for DS, causing their $\delta^{114/110}$Cd values deviating from the recommended values (Fig. S2†). Whereas for DSSA, matrix is reduced and diluted by adding pure standard solution, the separation of single column can make Sn/Cd decrease to less than 0.001 and achieve the expected results. Thus, DSSA simplify the purification process, greatly reducing reagents volume and shortening the separation time. Additionally, this also suggests that high-precision measurement of Cd isotopes in ultra-trace Cd samples can be performed without changing the instrument configuration or using higher-impedance Faraday cups (*e.g.*, $10^{12}/10^{13}$ Ω amplifier).

3.4. Application of DSSA to biological samples with ultra-trace Cd

Since the Cd content in biological samples is very low, more than 1 g sample is required to digest for isotope analysis. However, with the DSSA method, the largest sample size of our investigated biological samples was 2629 mg despite its Cd content is as low as 0.004 μg g^{-1} in oyster shell, approximately 1/5 of the requirement by the traditional DS[8] (Table 2). Reduced sample requirement allows us to investigate variations in the Cd concentrations and isotope compositions of animal organs. Cadmium contents in investigated animal organs are extremely low, with the order of liver (0.077 μg g^{-1}) ≈ kidney (0.076 μg g^{-1}) > lung (0.009 μg g^{-1}) in ovine and kidney (0.106 μg g^{-1}) > liver (0.020 μg g^{-1}) > lung (0.011 μg g^{-1}) in pig. The distribution trend of Cd in ovine and pig is consistent with that in mice,[48–50] suggesting enrichment of Cd in the kidney and liver of animals.

The $\delta^{114/110}$Cd values are 0.681 ± 0.027‰ (2SD, $n = 3$) for ovine kidney, 0.101 ± 0.051‰ (2SD, $n = 4$) for lung, and −0.054 ± 0.030‰ (2SD, $n = 3$) for liver. The $\delta^{114/110}$Cd of the pig kidney, lung, and liver are 0.370 ± 0.040‰ (2SD, $n = 22$), −0.009 ± 0.060‰ (2SD, $n = 3$), and 0.044 ± 0.044‰ (2SD, $n = 15$), respectively (Table 2 and Fig. S4†). Kidneys have the highest $\delta^{114/110}$Cd values among investigated organs, consistent with literature data for rats and pigs (0.635 ± 0.034‰[12] and 0.465 ± 0.062‰,[41] respectively). Ovine livers have the lowest $\delta^{114/110}$Cd values, with lungs falling between ovine kidneys and lungs, whereas Cd isotopes in pig livers are slightly heavier than pig lungs.

The main Cd source in animal kidneys and livers is dietary intake,[49] and previous studies indicated that Cd in these organs is primarily complexed with the sulfur group (–HS) of metallothionein.[48,51] The $\delta^{114/110}$Cd values of the ovine and pig kidneys are higher than those of plants such as flour (GBW08503C, 0.096 ± 0.042‰) or rice (0.175 ± 0.035‰). This may be explained by the metabolization of Cd through urine, during which isotopically light Cd preferentially binds to –HS in urine and isotopically heavy ones accumulate in the kidney.[28–30,52] Light Cd isotopes bound to –HS may be accumulated in livers due to the slowly metabolic rate of Cd with a biological half period of 10–30 years, resulting in Cd enrichment with slightly lighter Cd isotope signals than the initial intake.[55] However, the $\delta^{114/110}$Cd values of ovine livers are slightly lower than pig livers. This can be attributed to higher specific surface area and uptake rates in ovine livers, leading to more light Cd isotopes into ovine lives.[53,54] Besides, the pig livers have another free Cd^{2+} transport channel, that is, Cd^{2+} can enter pig livers through specific transport proteins.[54] Previous experiments have shown that free Cd^{2+} is isotopically heavier than Cd associated with transporter.[28,29] The $\delta^{114/110}$Cd values for the lung are within the aerosol range of −0.19–0.190‰,[56] indicating limited Cd isotope fractionation during Cd uptake by

the lung. The large differences in Cd isotope ratios among animal organs imply that Cd isotopes can potentially trace the biological processes of Cd in animals or humans, especially for the kidney and liver.

The Cd content in studied oyster shells is 0.004 μg g^{-1}. DSSA yields an average $\delta^{114/110}$Cd value of −0.591 ± 0.024‰ (Table 2, 2SD, $n = 4$), within the range of −1.20‰ to −0.09‰ for bivalves from French, American, and Atlantic Oceans.[57,58] The $\delta^{114/110}$Cd values of bivalves are significantly lower than those of the global ocean (~0.30‰),[20,21] indicating that carbonate shells preferentially take up light Cd isotopes from seawater. Thus, besides oceanic algae,[22] the evolution of carbonate biomineralization in Earth's history may have shaped Cd isotope composition of the seawater.

4. Conclusions

Using a series of certified GRMs and BRMs, including basalt, Mn-nodule, sediment, loss, plant, and human hair samples, we demonstrate the robustness of DSSA method for measuring the $\delta^{114/110}$Cd values in ultra-trace Cd samples with complex matrices and with as low as 2.09 ng of Cd. $\delta^{114/110}$Cd values derived from single- and multi-standard approaches are well consistent with recommended values, suggesting the robustness of both. However, if sample fraction (f_{spl}) is ≤15%, the precision can be up to 0.137‰ for single-standard addition and 0.199‰ for multi-standard addition. When f_{spl} is ≥20%, the overall precision, including single-standard and multi-standard, is 0.041 ± 0.022‰ (2SD, $n = 46$), indicating that 20–50% is the optimal mixing range to obtain high-precision Cd isotopes using as small sample masses as possible. The comparison between single- and multi-standard addition shows that there is no significant difference between the results, suggesting that DSSA can be operated simply by mixing sample with only one spiked secondary standard solution.

High accuracy and precision of DSSA in ultra-trace Cd samples allows for $\delta^{114/110}$ Cd measurement of a suite of animal organ samples with 0.004–0.106 μg g^{-1} Cd content with precisions better than 0.040‰. Large $\delta^{114/110}$ Cd variations among ovine and pig kidneys (0.681 ± 0.027‰ and 0.370 ± 0.040‰, respectively), livers (−0.054 ± 0.030‰ and 0.044 ± 0.044‰), and lungs (0.101 ± 0.051‰ and −0.009 ± 0.060‰) indicate that Cd isotopes might be used to trace metabolic processes. The $\delta^{114/110}$ Cd value of oyster shells is −0.591 ± 0.024‰ lower than global seawater values, implying that carbonate shells may be one of the crucial sinks of light Cd isotopes from the ocean.

Author contributions

H. C. and J.-M. Z. did writing – review & editing and visualization; J.-M. Z. made conceptualization, data curation, funding acquisition, resources and investigation; J.-M. Z. designed methodology; X. L. W. and T. G. did some writing – review& editing; J.-M. Z. was project administration and supervision. All authors contributed to the discussion and revision of the manuscript.

Conflicts of interest

There are no conflicts of interest to declare.

Acknowledgements

This work was financially supported by the National Key R&D Program of China (2019YFA0708400) and the National Natural Science Foundation of China (41973018 and 41673017). The authors thank Zhuo Lu (Ph.D candidate) for assistance with sample digestion, and Prof. Rehkämper at Imperial College London (ICL) and Dr Wombacher at University of Cologne for providing Münster Cd standard solution. We also appreciate the constructive comments and insightful suggestions of anonymous reviewers for improving paper quality, and Dr Gabriel Clarke for editorial handling.

References

1 J. Godt, F. Scheidig, C. Grosse-Siestrup, V. Esche, P. Brandenburg, A. Reich and D. A. Groneberg, The toxicity of cadmium and resulting hazards for human health, *J. Occup. Med. Toxicol.*, 2006, **1**(1), 22.
2 G. F. Nordberg, Historical perspectives on cadmium toxicology, *Toxicol. Appl. Pharmacol.*, 2009, **238**(3), 192–200.
3 E. A. Boyle, F. Sclater and J. M. Edmond, On the marine geochemistry of cadmium, *Nature*, 1976, **263**(5572), 42–44.
4 K. J. R. Rosman and J. R. De Laeter, The isotopic composition of cadmium in terrestrial minerals, *Int. J. Mass Spectrom. Ion Phys.*, 1975, **16**(4), 385–394.
5 K. J. R. Rosman and J. R. De Laeter, Isotopic fractionation in meteoritic cadmium, *Nature*, 1976, **261**(5557), 216–218.
6 F. Wombacher, M. Rehkämper, K. Mezger and C. Münker, Stable isotope compositions of cadmium in geological materials and meteorites determined by multiple-collector ICPMS, *Geochim. Cosmochim. Acta*, 2003, **67**(23), 4639–4654.
7 A.-D. Schmitt, S. J. G. Galer and W. Abouchami, High-precision cadmium stable isotope measurements by double spike thermal ionisation mass spectrometry, *J. Anal. At. Spectrom.*, 2009, **24**(8), 1079–1088.
8 D. Tan, J.-M. Zhu, X. Wang, G. Han, Z. Lu and W. Xu, High-sensitivity determination of Cd isotopes in low-Cd geological samples by double spike MC-ICP-MS, *J. Anal. At. Spectrom.*, 2020, **35**(4), 713–727.
9 Z. Lu, J.-M. Zhu, D. Tan, X. Wang and Z. Zheng, δ$^{114/110}$Cd values of a suite of different reference materials, *Geostand. Geoanal. Res.*, 2021, **45**(3), 565–581.
10 F. Wombacher and M. Rehkämper, Problems and suggestions concerning the notation of cadmium stable isotope compositions and the use of reference materials, *Geostand. Geoanal. Res.*, 2004, **28**(1), 173–178.
11 C. Cloquet, O. Rouxel, J. Carignan and G. Libourel, Natural cadmium isotopic variations in eight geological reference materials (NIST SRM 2711, BCR 176, GSS-1, GXR-1, GXR-2, GSD-12, Nod-P-1, Nod-A-1) and anthropogenic samples, measured by MC-ICP-MS, *Geostand. Geoanal. Res.*, 2005, **29**(1), 95–106.

12 N. Pallavicini, E. Engström, D. C. Baxter, B. Öhlander, J. Ingri and I. Rodushkin, Cadmium isotope ratio measurements in environmental matrices by MC-ICP-MS, *J. Anal. At. Spectrom.*, 2014, **29**(9), 1570–1584.

13 M.-S. Liu, Q. Zhang, Y. Zhang, Z. Zhang, F. Huang and H.-M. Yu, High-precision Cd isotope measurements of soil and rock reference materials by MC-ICP-MS with double spike correction, *Geostand. Geoanal. Res.*, 2020, **44**(1), 169–182.

14 X. Liu, L. Chen, H. Peng, G. Wang, N. Stanley, H. Zheng, S. Hu and Z. Zhu, Fast and highly sensitive Cd isotopic analyses in low-Cd complex samples with MC-ICP-MS based on plasma electrochemical vapor generation, *Anal. Chim. Acta*, 2022, **1215**, 339980.

15 B. Gao, Y. Liu, K. Sun, X. Liang, P. Peng, G. Sheng and J. Fu, Precise determination of cadmium and lead isotopic compositions in river sediments, *Anal. Chim. Acta*, 2008, **612**(1), 114–120.

16 T. M. Conway, A. D. Rosenberg, J. F. Adkins and S. G. John, A new method for precise determination of iron, zinc and cadmium stable isotope ratios in seawater by double-spike mass spectrometry, *Anal. Chim. Acta*, 2013, **793**, 44–52.

17 H. Peng, D. He, R. Guo, X. Liu, N. S. Belshaw, H. Zheng, S. Hu and Z. Zhu, High precision cadmium isotope analysis of geological reference materials by double spike MC-ICP-MS, *J. Anal. At. Spectrom.*, 2021, **36**(2), 390–398.

18 S. Ripperger, M. Rehkämper, D. Porcelli and A. N. Halliday, Cadmium isotope fractionation in seawater - a signature of biological activity, *Earth Planet. Sci. Lett.*, 2007, **261**(3–4), 670–684.

19 A. D. Schmitt, S. J. G. Galer and W. Abouchami, Mass-dependent cadmium isotopic variations in nature with emphasis on the marine environment, *Earth Planet. Sci. Lett.*, 2009, **277**(1–2), 262–272.

20 W. Abouchami, S. J. G. Galer, H. J. W. D. Baar, R. Middag, D. Vance, Y. Zhao, M. Klunder, K. Mezger, H. Feldmann and M. O. Andreae, Biogeochemical cycling of cadmium isotopes in the Southern Ocean along the Zero Meridian, *Geochim. Cosmochim. Acta*, 2014, **127**, 348–367.

21 R. C. Xie, S. J. G. Galer, W. Abouchami, M. J. A. Rijkenberg, H. J. W. de Baar, J. De Jong and M. O. Andreae, Non-Rayleigh control of upper-ocean Cd isotope fractionation in the western South Atlantic, *Earth Planet. Sci. Lett.*, 2017, **471**, 94–103.

22 D. J. Janssen, W. Abouchami, S. J. G. Galer, K. B. Purdon and J. T. Cullen, Particulate cadmium stable isotopes in the subarctic northeast Pacific reveal dynamic Cd cycling and a new isotopically light Cd sink, *Earth Planet. Sci. Lett.*, 2019, **515**, 67–78.

23 S. V. Georgiev, T. J. Horner, H. J. Stein, J. L. Hannah, B. Bingen and M. Rehkämper, Cadmium-isotopic evidence for increasing primary productivity during the Late Permian anoxic event, *Earth Planet. Sci. Lett.*, 2015, **410**, 84–96.

24 S. V. Hohl, S.-Y. Jiang, H.-Z. Wei, D.-H. Pi, Q. Liu, S. Viehmann and S. J. G. Galer, Cd isotopes trace periodic (bio)geochemical metal cycling at the verge of the Cambrian animal evolution, *Geochim. Cosmochim. Acta*, 2019, **263**, 195–214.

25 R. Frei, L. Xu, J. A. Frederiksen and B. Lehmann, Signals of combined chromium–cadmium isotopes in basin waters of the Early Cambrian – Results from the Maoshi and Zhijin sections, Yangtze Platform, South China, *Chem. Geol.*, 2021, **563**, 120061.

26 M. Sieber, T. M. Conway, G. F. D. Souza, C. S. Hassler, M. J. Ellwood and D. Vance, High-resolution Cd isotope systematics in multiple zones of the Southern Ocean from the Antarctic Circumnavigation Expedition, *Earth Planet. Sci. Lett.*, 2019, **527**, 115799.

27 Y. Liu, Y. Xia, Z. Wang, T. Gao, J.-M. Zhu, M. Qi, J. Sun and C. Liu, Lithologic controls on the mobility of Cd in mining-impacted watersheds revealed by stable Cd isotopes, *Water Res.*, 2022, **220**, 118619.

28 M. Wiggenhauser, M. Bigalke, M. Imseng, M. Müller, A. Keller, K. Murphy, K. Kreissig, M. Rehkämper, W. Wilcke and E. Frossard, Cadmium isotope fractionation in soil–wheat systems, *Environ. Sci. Technol.*, 2016, **50**(17), 9223–9231.

29 M. Imseng, M. Wiggenhauser, A. Keller, M. Müller, M. Rehkämper, K. Murphy, K. Kreissig, E. Frossard, W. Wilcke and M. Bigalke, Towards an understanding of the Cd isotope fractionation during transfer from the soil to the cereal grain, *Environ. Pollut.*, 2019, **244**, 834–844.

30 M. Wiggenhauser, A. M. Aucour, S. Bureau, S. Campillo, P. Telouk, M. Romani, J. F. Ma, G. Landrot and G. Sarret, Cadmium transfer in contaminated soil-rice systems: Insights from solid-state speciation analysis and stable isotope fractionation, *Environ. Pollut.*, 2021, **269**, 115934.

31 S. Zhong, X. Li, F. Li, Y. Huang, T. Liu, H. Yin and J. Qiao, Cadmium uptake and transport processes in rice revealed by stable isotope fractionation and Cd-related gene expression, *Sci. Total Environ.*, 2022, **806**, 150633.

32 H. Pickard, E. Palk, M. Schönbächler, R. E. T. Moore, B. J. Coles, K. Kreissig, K. Nilsson-kerr, S. J. Hammond, E. Takazawa, C. Hémond, P. Tropper, D. N. Barfod and M. Rehkämper, The cadmium and zinc isotope compositions of the silicate Earth – implications for terrestrial volatile accretion, *Geochim. Cosmochim. Acta*, 2022, **338**, 165–180.

33 W. F. McDonough and S. Sun, The composition of the Earth, *Chem. Geol.*, 1995, **120**(3), 223–253.

34 S. R. Taylor and S. M. McLennan, The geochemical evolution of the continental crust, *Rev. Geophys.*, 1995, **33**(2), 241–265.

35 R. L. Rudnick and S. Gao, *Composition of the continental crust*, Elsevier, Oxford, 2014, pp. 1–51.

36 G. Witt-eickschen, H. Palme, H. S. C. O. Neill and C. M. Allen, The geochemistry of the volatile trace elements As, Cd, Ga, In and Sn in the Earth's mantle: new evidence from in situ analyses of mantle xenoliths, *Geochim. Cosmochim. Acta*, 2009, **73**(6), 1755–1778.

37 WHO, *Exposure to Cadmium: a Major Public Health Concern*, World Health Organization, Geneva, 2010, pp. 1–6.

38 United Nations Environment Programme (UNEP), *Final Review of Scientific Information on Cadmium*, 2010, pp. 3–201.

39 M. Satoh, H. Koyama, T. Kaji, H. Kito and C. Tohyama, Perspectives on cadmium toxicity research, *J. Exp. Med.*, 2002, **196**(1), 23–32.
40 M. Uetani, E. Kobayashi, Y. Suwazono, R. Honda, M. Nishijo, H. Nakagawa, T. Kido and K. Nogawa, Tissue cadmium (Cd) concentrations of people living in a Cd polluted area, Japan, *BioMetals*, 2006, **19**(5), 521–525.
41 J. Borovička, L. Ackerman and J. Rejšek, Cadmium isotopic composition of biogenic certified reference materials determined by thermal ionization mass spectrometry with double spike correction, *Talanta*, 2021, **221**, 121389.
42 Z. Xue, M. Rehkämper, M. Schönbächler, P. J. Statham and B. Coles, A new methodology for precise cadmium isotope analyses of seawater, *J. Anal. Bioanal. Chem.*, 2012, **402**(2), 883–893.
43 G. Wu, J. M. Zhu, X. Wang, T. M. Johnson and G. Han, High-sensitivity measurement of Cr isotopes by double spike MC-ICP-MS at the 10 ng Level, *Anal. Chem.*, 2020, **92**(1), 1463–1469.
44 Z. Lu, J. M. Zhu, D. Tan, T. M. Johnson and X. Wang, Double spike-standard addition technique and its application in measuring isotopes, *Anal. Chem.*, 2023, **95**(4), 2253–2259.
45 J. M. Zhu, G. Wu, X. Wang, G. Han and L. Zhang, An improved method of Cr purification for high precision measurement of Cr isotopes by double spike MC-ICP-MS, *J. Anal. At. Spectrom.*, 2018, **33**(5), 809–821.
46 R. Schoenberg, S. Zink, M. Staubwasser and F. von Blanckenburg, The stable Cr isotope inventory of solid Earth reservoirs determined by double spike MC-ICP-MS, *Chem. Geol.*, 2008, **249**(3), 294–306.
47 D. Li, M.-L. Li, W.-R. Liu, Z.-Z. Qin and S.-A. Liu, Cadmium isotope ratios of standard solutions and geological reference materials measured by MC-ICP-MS, *Geostand. Geoanal. Res.*, 2018, **42**(4), 593–605.
48 T. Zeng, R. Zhang, Y. Chen, W. Guo, J. Wang and Z. Cai, In situ localization of lipids on mouse kidney tissues with acute cadmium toxicity using atmospheric pressure-MALDI mass spectrometry imaging, *Talanta*, 2022, **245**, 123466.
49 H. Zhang, J. Yan, Y. Xie, X. Chang, J. Li, C. Ren, J. Zhu, L. Ren, K. Qi, Z. Bai and X. Li, Dual role of cadmium in rat liver: inducing liver injury and inhibiting the progression of early liver cancer, *Toxicol. Lett.*, 2022, **355**(1), 62–81.
50 Y. T. Tai, S. H. Chou, C. Y. Cheng, C. Te Ho, H. C. Lin, S. M. Jung, P. H. Chu and F. H. Ko, The preferential accumulation of cadmium ions among various tissues in mice, *Toxicol. Rep.*, 2022, **9**, 111–119.
51 L. L. Needham, P. Grandjean, B. Heinzow, P. J. Jørgensen, F. Nielsen, A. Sjödin, D. G. Patterson, W. E. Turner and P. Weihe, Partition of environmental chemicals between maternal and fetal blood and tissues, *Environ. Sci. Technol.*, 2011, **45**(3), 1121–1126.
52 Y. Zhao, Y. Li, M. Wiggenhauser, J. Yang, G. Sarret, Q. Cheng, J. Liu and Y. Shi, Theoretical isotope fractionation of cadmium during complexation with organic ligands, *Chem. Geol.*, 2021, **571**(19), 120178.
53 C. J. C. Phillips and L. Tudoreanu, A model of cadmium accumulation in the liver and kidney of sheep derived from soil and dietary characteristics, *J. Sci. Food Agric.*, 2011, **91**(2), 370–376.
54 V. M. Tomović, L. S. Petrović, M. S. Tomović, Ž. S. Kevrešan, M. R. Jokanović, N. R. Džinić and A. R. Despotović, Cadmium concentrations in the liver of 10 different pig genetic lines from Vojvodina, Serbia, *Food Addit. Contam., Part B*, 2011, **4**(3), 180–184.
55 D. Elez, J. Dundjerski and G. Matić, Cadmium affects the redox state of rat liver Glucocorticoid Receptor, *Cell Biol. Toxicol.*, 2001, **17**(3), 169–177.
56 L. Bridgestock, M. Rehkämper, T. van de Flierdt, K. Murphy, R. Khondoker, A. R. Baker, R. Chance, S. Strekopytov, E. Humphreys-Williams and E. P. Achterberg, The Cd isotope composition of atmospheric aerosols from the Tropical Atlantic Ocean, *Geophys. Res. Lett.*, 2017, **44**(6), 2932–2940.
57 A. E. Shiel, D. Weis and K. J. Orians, Tracing cadmium, zinc and lead sources in Bivalves from the Coasts of Western Canada and the USA using isotopes, *Geochim. Cosmochim. Acta*, 2012, **76**, 175–190.
58 A. E. Shiel, D. Weis, D. Cossa and K. J. Orians, Determining provenance of marine metal pollution in French Bivalves using Cd, Zn and Pb isotopes, *Geochim. Cosmochim. Acta*, 2013, **121**, 155–167.

